ACOUSTIC NONDESTRUCTIVE TESTING OF STEEL REINFORCING MEMBERS IN CONCRETE

Michael K. McInerney*, Sean W. Morefield, Vincent F. Hock
U.S. Army Engineer Research and Development Center, Construction Engineering Research Laboratory
Champaign, Illinois 61822

John M. Carlyle
Carlyle Consulting
Yardley, Pennsylvania 19067

ABSTRACT

Many concrete structures contain internal pre- and post-tensioned steel structural members that are subject to fracturing and corrosion. Corrosion of steel components can lead to loss of tension and consequent severe problems, such as cracking of the concrete or fracturing of the steel. This work addresses the problem of determining tension in embedded pre- and post-tensioned rods. The major problem with existing test techniques is that they use indirect and non-quantitative methods to determine whether there has been a loss of tension. We have developed an acoustic technique and sensor to make quantitative tension measurements in an embedded tensioned steel member. Although initially developed for civil works applications, this new acoustic technique is directly applicable to any concrete structure with steel members in tension, including bridges and heavily reinforced bunkers.

Acoustic technology provides a method to measure the tension quickly, accurately, and quantitatively. Researchers at ERDC-CERL developed a theory and measurement technique for determining tensile stress in steel directly from ultrasonic measurements, and a procedure to simulate the ultrasonic environment inside a steel rod. An invention disclosure has been submitted on this acoustic technology.

From fundamental physical laws of materials, we have derived a scheme for relating tension to a material's acoustic properties. An ultrasonic propagation model was developed to predict wave propagation and to help make tension field measurements easier. Laboratory evaluation of the technique and verification of the theory has been conducted. We observed excellent agreement between our simulation and tests on actual tensioned rods. Field trials at two U.S. Army Corps of Engineers lock and dam facilities proved that the technique could indeed measure tension in rods up to 50 feet long, and the ultrasonically measured values were within 4% of the mechanically measured values.

1. INTRODUCTION

1.1 Background

Acoustic waves are nondestructive, are capable of traveling long distances in engineered structures, and can thoroughly interrogate a structure's integrity. Acoustics are dual purpose – they can determine bulk material properties, such as tension, by using signals that interact macroscopically with the material, as well as detect small defects, such as fractures, by using signals that interact microscopically with the material. This dual nature is achieved by using different acoustic signal processing techniques on the signals received after a carefully shaped signal is launched into the material. Measurements can be performed very quickly, usually in real-time (although processing might extend this by one or two minutes).

1.2 Objective

The research objective was to develop a theory and test technique for quantitatively determining tension in embedded steel members.

1.3 Approach

The first step was to establish the theoretical basis behind bulk tension measurements. In the second step, an acoustic propagation model was developed and implemented using commercially available software. An instrument and a dual ultrasonic mode sensor were designed. Sample steel rods were also fabricated that could be inserted into a hydraulic tensioning device, and laboratory experiments were performed o prove that we could make tension measurements using acoustic techniques.

Report Documentation Page

Form Approved
OMB No. 0704-0188

Public reporting burden for the collection of information is estimated to average 1 hour per response, including the time for reviewing instructions, searching existing data sources, gathering and maintaining the data needed, and completing and reviewing the collection of information. Send comments regarding this burden estimate or any other aspect of this collection of information, including suggestions for reducing this burden, to Washington Headquarters Services, Directorate for Information Operations and Reports, 1215 Jefferson Davis Highway, Suite 1204, Arlington VA 22202-4302. Respondents should be aware that notwithstanding any other provision of law, no person shall be subject to a penalty for failing to comply with a collection of information if it does not display a currently valid OMB control number.

1. REPORT DATE **01 DEC 2008**	2. REPORT TYPE **N/A**	3. DATES COVERED **-**
4. TITLE AND SUBTITLE **Acoustic Nondestructive Testing Of Steel Reinforcing Members In Concrete**		5a. CONTRACT NUMBER 5b. GRANT NUMBER 5c. PROGRAM ELEMENT NUMBER
6. AUTHOR(S)		5d. PROJECT NUMBER 5e. TASK NUMBER 5f. WORK UNIT NUMBER
7. PERFORMING ORGANIZATION NAME(S) AND ADDRESS(ES) **U.S. Army Engineer Research and Development Center, Construction Engineering Research Laboratory Champaign, Illinois, 61822**		8. PERFORMING ORGANIZATION REPORT NUMBER
9. SPONSORING/MONITORING AGENCY NAME(S) AND ADDRESS(ES)		10. SPONSOR/MONITOR’S ACRONYM(S) 11. SPONSOR/MONITOR’S REPORT NUMBER(S)

12. DISTRIBUTION/AVAILABILITY STATEMENT
Approved for public release, distribution unlimited

13. SUPPLEMENTARY NOTES
See also ADM002187. Proceedings of the Army Science Conference (26th) Held in Orlando, Florida on 1-4 December 2008, The original document contains color images.

14. ABSTRACT

15. SUBJECT TERMS

16. SECURITY CLASSIFICATION OF:			17. LIMITATION OF ABSTRACT	18. NUMBER OF PAGES	19a. NAME OF RESPONSIBLE PERSON
a. REPORT **unclassified**	b. ABSTRACT **unclassified**	c. THIS PAGE **unclassified**	**UU**	**8**	

Standard Form 298 (Rev. 8-98)
Prescribed by ANSI Std Z39-18

Field tests were conducted at two U.S. Army Corps of Engineers dams, located in Oklahoma and Georgia.

2. THEORETICAL BACKGROUND

2.1 Basic Ultrasonic Theory

A material's ultrasonic properties are fundamental to the understanding of wave behavior. Ultrasonic waves propagate as both longitudinal and shear waves. The two different wave propagations are displayed in Figure 1, and Table 1 gives some of the more important ultrasonic properties of common structural materials.

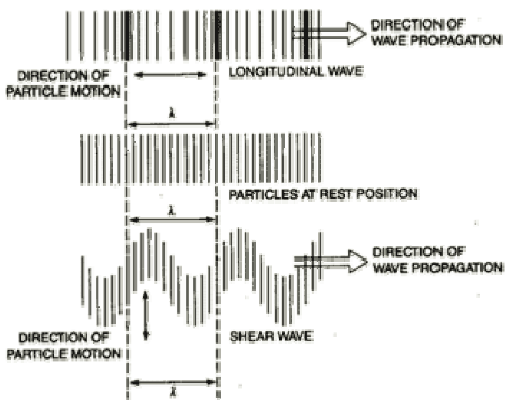

Figure 1. Illustration of acoustic wave propagation.

Table I Published Material Properties

	Longitudinal Velocity, V_l (cm/μS)	Shear Velocity, V_s (cm/μS)	Density, ρ (gm/cm^3)	Acoustic Impedance, Z (g/cm^{2}S x 10^6)
Air	0.034	None	1.21 x 10^{-3}	4.15 x 10^{-5}
Aluminum	0.632	0.313	2.73	1.725
Concrete	0.432	--	2.60	1.123
Granite	0.395	--	2.75	1.086
Perspex	0.276	0.143	1.19	0.328
Steel	0.585	0.323	7.80	4.563
Water	0.148	None	1.00	0.148

Important interaction aspects of ultrasonic waves include transmission and reflection at interfaces. This knowledge provides for an understanding of whether or not the sound will stay within the confines of the object. The angles that waves take upon encountering boundaries are important for understanding where the various modes of sound will propagate in a component. Also, the spreading of ultrasound from a sensor is important for understanding if there will be enough energy received to make a tension measurement.

The information in Table 1 allows us to find the transmission, α_t, and reflection, α_r, coefficients at interfaces. Equations 1 and 2 provide a formula to calculate each coefficient.

$$\alpha_t = \frac{4\rho_1V_1\rho_2V_2}{(\rho_1V_1+\rho_2V_2)^2} = \frac{4Z_1Z_2}{(Z_1+Z_2)} \qquad (1)$$

$$\alpha_r = \left[\frac{(\rho_2V_2-\rho_1V_1)}{(\rho_1V_1+\rho_2V_2)}\right]^2 = \left[\frac{(Z_2-Z_1)}{(Z_1+Z_2)}\right]^2 \qquad (2)$$

ρ_1 is the density of medium 1, ρ_2 is the density of medium 2, V_1 is the velocity in medium 1, V_2 is the velocity in medium 2, Z_1 is the acoustic impedance of medium 1 and Z_2 is the acoustic impedance of medium 2.

Figure 2 illustrates wave transmission and reflection angles between media. Snell's Law relates these angles to the properties of the acoustic media.

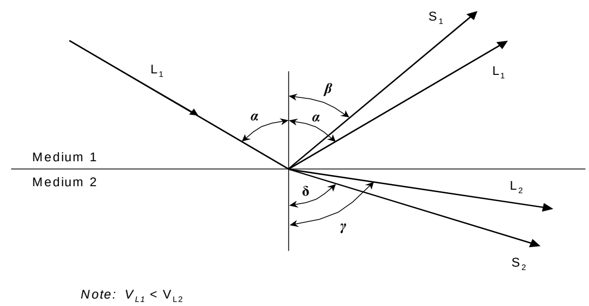

Figure 2. Illustration of wave transmission and reflection at medium boundary.

Snell's Law, shown in Equation 3, gives us the ability to determine the angle at which a reflected ultrasonic wave will travel, given the speed of sound of the wave mode in the medium. Equation 4 is a rearrangement of Snell's Law.

$$\frac{\sin\alpha}{V_{l1}} = \frac{\sin\beta}{V_{s1}} = \frac{\sin\gamma}{V_{l2}} = \frac{\sin\delta}{V_{s2}} \qquad (3)$$

$$\gamma = \arcsin(\sin\frac{\alpha V_2}{V_1}) \qquad (4)$$

V_{l1} is the velocity of the longitudinal wave in medium 1, V_{s1} is the velocity of the shear wave in medium 1, V_{l2} is the velocity of the longitudinal wave in medium 2, V_{s2} is the velocity of the shear wave in medium 2, α is the angle from a perpendicular to the boundary surface to the propagation direction of the longitudinal wave in medium 1, β is the angle from a perpendicular to the boundary surface to the propagation direction of the shear wave in medium 1, γ is the angle from a perpendicular to the boundary surface to the propagation direction of the longitudinal wave in medium 2, and δ is the angle from a perpendicular to

the boundary surface to the propagation direction of the shear wave in medium 2.

The ultrasonic wave energy emitted from a sensor spreads in a conical shape as it travels, thus decreasing its energy per unit area. The far field is approximated by a distance 2a/λ or farther from the sensor, where a is the sensor's aperture radius and λ is the wavelength. Because we are working with long rods, we need to know how the ultrasonic beam behaves, far from the sensor. Equation 5 allows us to calculate the divergence angle, θ, of an ultrasonic beam in the far field.

$$\theta = \arcsin(k\lambda / 2a) \qquad (5)$$

where k is a constant with a value of 0.5 or 0.6, and λ is the wavelength of the ultrasound. It is also important to note that the beam energy exhibits a sinusoidal pattern. The energy is focused toward the center of the beam, and dissipates as it gets to the edges.

2.2 Tension Measurement Theory

Given equations describing linear elastic deformation and ultrasonic wave speed (such as those shown in Figure 3), an equation describing how to determine tension inside a material using pure ultrasonic measurements can be derived. The elastic deformation quantities include Hooke's Law, the Bulk Modulus, Young's Modulus, the Shear Modulus, and Poisson's Ratio. Using the seven equations given in Figure 3, we obtain Equation 6 that relates tension to pure ultrasonic properties, the velocities of the longitudinal and shear waves.

$$\sigma \propto \left(v_l^2 - 2v_s^2\right) / 2\left(v_l^2 - v_s^2\right) \qquad (6)$$

Hooke's Law

$$\sigma_{ij} = \lambda\, \delta_{ij}\, \varepsilon_{aa} + 2\, \mu\, \varepsilon_{ij}$$

Young's Modulus

$$E = \mu\, (3\lambda + 2\mu) / (\lambda + \mu) = \sigma_{zz} / \varepsilon_{zz}$$

Bulk Modulus

$$K = \lambda + 2\mu / 3 = \sigma_{xx} / (3\, \varepsilon_{xx}) = \sigma_{yy} / (3\, \varepsilon_{yy}) = \sigma_{zz} / (3\, \varepsilon_{zz})$$

Shear Modulus

$$\sigma_{zx} = 2\, \mu\, \varepsilon_{zx}$$

Poisson's Ratio

$$\nu = \lambda / 2(\lambda + \mu)$$

Longitudinal Wave Speed

$$V_l = (c_{11} / \rho)^{1/2}$$

Shear Wave Speed

$$V_s = (c_{44} / \rho)^{1/2}$$

Figure 3. Fundamental laws and equations governing material properties.

3. ULTRASONIC SIMULATION

3.1 Simulation Software

The Imagine3D® software package, sold by Utex Scientific Instruments, Inc., assists engineers in specifying transducer characteristics needed to inspect complex parts. A hypothesis was made that Imagine3D® could be used to extend the tension measurement theory into actual working models. The software's performance was checked against actual measurements made using an ultrasonic instrument, and its feasibility as a modeling environment was verified.

3.2 Modeling a Steel Rod

During the second phase of the work , Imagine3D® was used to model a 19-inch-long plain steel rod, measuring 1.25 inches in diameter. This seemingly simple object actually involves a great deal of complexity, due to beam divergence and mode conversion[1], and allowed us to check the validity of Imagine3D® as a modeling environment.

The experimental setup and the acoustic wave propagation simulation of the rod are shown in Figure

[1] conversion from a longitudinal to a shear wave and vice versa

4. As can be seen, the sensor is mounted on the left-hand face of the rod. The sound travels down the rod, reflects off the right hand face of the rod, and travels back to the sensor. Not obvious is the fact that the beam from the sensor is diverging as it travels. The beam divergence is clearly shown in the bottom plot of Figure 4, where the blue rays coming from the sensor have a clear conical shape. As the beam interacts with the side of the rod it reflects and mode-converts in accordance with Snell's Law. The reflected ultrasonic rays are shown in green. Because of the number of rays involved, the reflected beam seems to fill the rod, but in reality each ray is traveling at an angle to the surface of the rod (as it must). Mode conversion is also taking place when the side reflection occurs, and although the simulator is producing rays that correspond to shear waves, we do not see them in the simulation view we have chosen.

Figure 5 shows the results of the beam divergence and the mode conversion that is taking place inside the steel rod when the simulator sums all of the echoes received from the rod. The rod is 19 inches long, and, as expected, there is a strong echo that appears at 19 inches. This is caused by the longitudinal wave traveling straight down the rod, reflecting off of the right hand face, and traveling back to the sensor.

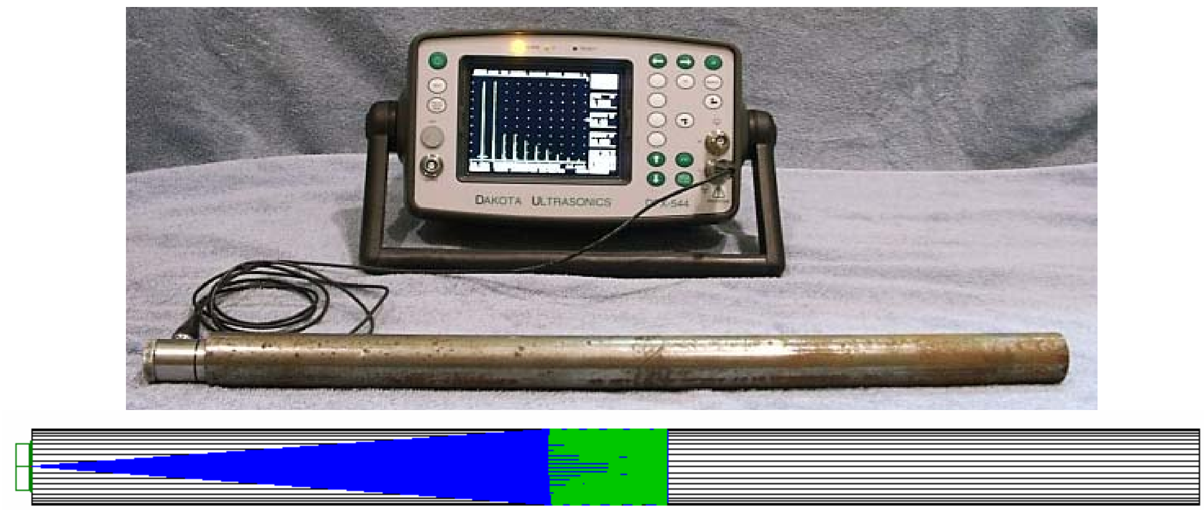

Figure 4. (Top) Ultrasonic instrument showing received signal from sensor on side of rod. (Bottom) Model of sensor on rod, clearly showing beam spread (blue) as ultrasound travels into rod. Reflections off side of rod are in green

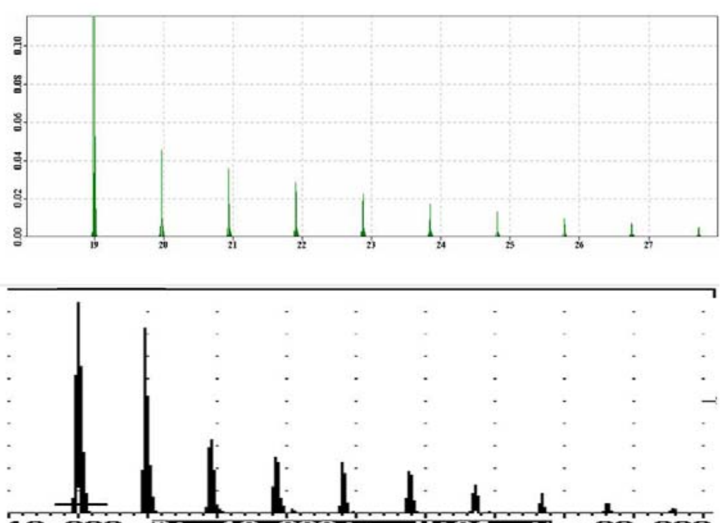

Figure 5. (Top) Imagine3D® simulation of echoes produced in a steel rod. (Bottom) Actual screen shot from ultrasonic instrument.

But there are other echoes, too, that appear after 19 inches. These echoes are caused by the mode conversion of the original longitudinal ultrasonic beam into shear waves, as the diverging beam interacts with the sides of the rod. Since shear waves travel only half as fast as longitudinal waves, when they eventually arrive back at the sensor they will lag behind the faster “directly there and directly back” longitudinal beam. As can be seen, the agreement between the simulation and the result obtained from the real instrument is very good.

In addition to placing all of the echoes at the proper distance, Imagine3D® also does a good job of calculating the expected amplitude for the echoes. The only real disagreement between the result obtained from the real instrument and simulation appears in the echo at 20 inches. In the real instrument, this particular echo had more strength than predicted by simulation. The other echoes, at about 21, 22, 23, 24, 25, 26, 27 and 28 inches, agreed very well. We can conclude that Imagine3D® did a very good job in simulating this complex situation.

4. TENSION MEASUREMENTS USING ULTRASOUND

The key to measuring tension in a component is to obtain the necessary ultrasonic measurements with a high degree of accuracy. There are two ways to do this: (1) the simulator can be used to obtain the necessary measurements from two echoes, thus enabling the calculation of tension in components; (2) a special sensor (described in an invention disclosure) can be used to make the necessary ultrasonic measurements directly (and potentially, more accurately).

4.1 Simulating Tension Measurements

The tension measurement model we have developed is composed of an equation together with the accurate ultrasonic echo modeling capabilities of Imagine3D®. Our equation calculates a material’s bulk stress, σ, in terms of ultrasonic quantities. This equation permits us to measure the tension in an embedded steel rod, such as a tainter gate anchor rod, by determining two ultrasonic properties and dividing the calculated stress value by the circular area of the rod. The physical changes produced by tension in a rod can be determined using the isotropic version of Hooke's Law, $E = \sigma_{zz} / \varepsilon_{zz}$. Stress, σ, is force (tension) divided by area, while strain, ε, is change in length divided by the original length. We can derive the following relationship for the length change that results from a given tension in a rod.

$$\Delta L = {F\,L}/{A\,E} \qquad (7)$$

where *F* is the applied force, *L* is the original length of the rod, A is the circular area of the rod and E is Young's modulus. The change in length for various applied loads to a 19-inch-long plain steel rod, having a 1.25 inch diameter, are calculated using equation 7 and presented in Table 2.

Table 2. Load-Induced Length Change in a 19 inch Long by 1.25 inches Diameter Steel Rod

Load	Length Change
100 pounds	0.000525 inches
500 pounds	0.002627 inches
1000 pounds	0.005253 inches
5000 pounds	0.026267 inches
10000 pounds	0.052534 inches

Using the information in Table 2, the simulator can be used to predict the exact position of the ultrasonic echoes that will result when the length of the 19-inch-steel rod is increased by these different lengths. Thus, we can see directly the effect of tension on ultrasound echoes in the steel bar. This accomplishes two things: (1) it permits us to see the magnitude change of any given tension state and (2) it permits us to see the effect of tension on any particular echo. The first point is important because it allows us to determine the precision with which the ultrasonic velocity measurements will have to be conducted. The second point is even more important, although the reason is a little less obvious.

The echoes shown in Figure 6 are produced in Imagine3D® by specifying the wave modes that can exist in the rod. The first echo, at 19 inches, is the result of a longitudinal wave propagating down the length of the rod and another longitudinal wave reflecting off of the back surface and returning to the sensor. This can be seen clearly in the top and bottom plots of Figure 6; the blue rays are the longitudinal wave propagating down the length of the rod and the green rays correspond to this longitudinal wave, reflecting off the back surface and returning to the sensor. Note that there are no shear waves in the first echo.

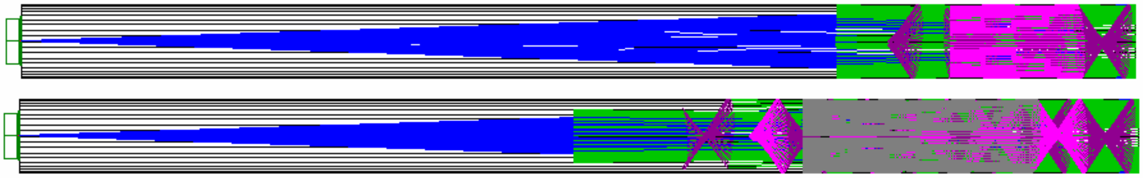

Figure 6. (Top) Model of 19 inch long by 1.25 inches diameter steel rod, showing how 1st echo (green rays) and 2nd echo (light purple rays) are formed. (Bottom) Model showing how the 1st echo (green rays) and 3rd echo (gray rays) are formed.

However, the second, third, and higher echoes are composed of a mix of longitudinal waves and shear waves. The top plot of Figure 6 shows how the second echo is created. A longitudinal wave (blue) propagates down the rod, a reflected longitudinal wave (green) comes off the back surface, and a reflected shear wave (dark purple) is created when the reflected longitudinal wave mode-converts when it hits the side of the rod. Another reflected longitudinal wave (light purple) is created when this shear wave mode-converts on the other side of the rod. This last longitudinal wave returns to the sensor to create echo 2. This event can be expressed with the following equation for the time of echo 2, t_{e2}.

$$t_{e2} = \frac{x_2}{V_l} + \frac{x_3}{V_l} + \frac{x_4}{V_s} + \frac{x_5}{V_l} \qquad (8)$$

where V_l and V_s are the longitudinal wave speed and the shear wave speed, respectively, and x_2, x_3, x_4, and x_5 are the path lengths for the appropriate rays in the rod.

Similarly, the bottom plot of Figure 6 shows how the third echo is created. A longitudinal wave (blue) propagates down the rod and a reflected longitudinal wave (green) comes off of the back surface. A reflected shear wave (dark purple) is created when the reflected longitudinal wave mode-converts when it hits the side of the rod and another reflected shear wave (light purple) is created when the first reflected shear wave reflects off of the other side of the rod. Finally a reflected longitudinal wave (gray) is created when this second shear wave mode-converts on the other side of the rod. This last longitudinal wave returns to the sensor to create echo 3. This can be expressed with the following equation for the time of echo 3, t_{e3},.

$$t_{e3} = \frac{x_2}{V_l} + \frac{x_3}{V_l} + \frac{x_6}{V_s} + \frac{x_7}{V_l} \qquad (9)$$

where V_l and V_s are the longitudinal wave speed and the shear wave speed, respectively, and x_2, x_3, x_4, x_6, and x_7 are the path lengths for the appropriate rays in the rod.

Imagine3D® will thus provide the measurements of the ultrasonic quantities that we need to obtain the predicted value for the tension in the simulated rod. This is exactly the tension measurement model that we have been seeking.

4.2 Acoustic Measurements of Tension

Laboratory tests were first conducted on a 19-inch-long plain steel rod, with a diameter of 1.25 inches. This allowed us to check the validity of the equations and the measurement technique. The acoustic transducer is mounted on the part being tested, using an ultrasonic couplant, and the velocities of the longitudinal and shear waves are measured. In these laboratory experiments, good agreement was obtained between direct tension measurement and the tension calculated from acoustic measurements.

We have completed two field tests with the Acoustic NDT instrument, both at U.S. Army Corps of Engineers dams, one located in Georgia and one in Oklahoma. Tension measurements were taken on trunnion anchorage anchor rods.

Trunnion anchorages are large concrete blocks that anchor the tainter gate trunnions to the dam. (The trunnions are the giant pivots that the tainter gates are attached to.) The concrete anchorages are bolted to the dam with large steel rods that extend through the anchorages and into the piers of the dam.

Figure 7 is a photograph of tainter gates and trunnions at one of the test locations. In this picture, the anchor rods are located behind vertical rectangular steel covers (Figure 8). In Figure 9, the cover has been removed for anchor rod testing.

Figure 7. Tainter gates and trunnions.

Figure 8. Anchor rod covers and a failed anchor rod that shot through the cover.

Figure 9. Cover removed exposing anchor rods prior to testing.

The rods are post-tensioned, following installation of the concrete anchorages.

The first field test was conducted on a dam Oklahoma. Twenty rods on Pier 3 were randomly selected for testing (out of a total of 56 rods on that pier). All rods were 50 feet in length. All ends were smoothed on the inside of the dam, but on the outside of the dam, only ten ends were smoothed (leaving the remaining ten on the outside with rough flame-cut ends). This resulted in a total of ten rods with good ultrasonic reflectors on the far end (testing was done from the inside of the dam), and ten with poor far-end ultrasonic reflectors. Testing showed that longitudinal ultrasound propagated through only six of the twenty rods (five were smooth on both ends, while one was smooth on only one end). Shear ultrasound propagated through only one rod (which was smooth on both ends). This meant that tension calculations could be made for only one of the 50-foot rods. For this rod, the tension was calculated as a load of 90,359 lbs and a tension of 56,251 psi. The design specifications called for a load of 86,500 lbs, giving an experimental error of only 4%. It wasn't apparent why the two required modes of ultrasound propagated through only one of the rods.

Previous laboratory experiments on a failed 36-foot rod, that had been removed from another dam, showed there was plenty of signal (about 46 dB gain remained). The system was calibrated using this rod. One explanation for the increased attenuation is that the metallurgy of these rods is slightly different. Some improvements in signal were obtained onsite at Keystone by careful polishing of the rod ends.

The second field test was conducted at a dam in Georgia. Thirty-eight rods on Pier E were tested. These rods were 38 to 48 feet in length, and both longitudinal and shear ultrasonic signals were obtained for all rods. We are still looking over the drawings and specifications to verify rod lengths, initial loads, and material characteristics. However, qualitatively, the measurements are consistent. The two rods that showed an increase in loading over their original tensioning are in locations where they will receive extra loading due to a broken rod. Overall, the generally lower load readings could simply be due to 40 years of creep. However, this is just speculation. A detailed engineering analysis will confirm if this is probable.

CONCLUSIONS

A means of measuring tension ultrasonically was developed, and an invention disclosure on the new method was submitted. From fundamental physical laws of materials, a scheme for relating tension to ultrasonic quantities was derived. In addition, an ultrasonic simulator was developed to predict wave

propagation and to help make tension field measurements easier. Excellent agreement was observed between both the simulation and the tests on real test rods. A unique sensor was developed to make the tension measurement more accurate in the field, and a prototype instrument was developed. Both laboratory evaluation of the instrument and verification of the theory are presently being conducted.

We tested twenty trunnion anchorage anchor rods at a dam in Oklahoma, but were able to reliably measure the tension in only one. On the majority of the rods, the acoustic signal was too weak to sense (these were 55-foot rods), leading us to conclude that the present technique was most effective on shorter rods. A dam in Georgia was chosen for our second field test because it had shorter rods, and because they had an ongoing rod inspection project. We took measurements on 38 rods at this site, and were able to measure a signal on each one; although the quality and consistency of the signal varied. This led to variability in the computed rod tensions. When compared to the last tension measurements (by jacking), a couple were right on, some were slightly off, and some were way off. We're currently analyzing this data to determine which parameter is causing this variability.

The benefits of this technique, when fully developed, are:

- ability to rapidly measure tension of embedded steel rods in the field,
- only limited access to the rod is required, one or both ends, and
- a cost savings of at least a factor of ten over the present lift-off testing method.

Ease and inexpensiveness of this NDT technology will allow for more testing and improved structural evaluation.

Although initially developed for civil works applications, this new acoustic technique is directly applicable to any structure with steel members in tension, including bridges and heavily reinforced bunkers.

ACKNOWLEDGMENT

The authors would like to thank district and division personnel of the U.S. Army Corps of Engineers for their assistance in conducting field tests at two Corps of Engineer dams.

REFERENCES

Auld, B.A., 1990: *Acoustic Fields and Waves in Solids*, Vol I & II, 2d edition, Krieger Publishing Company,878 pp.

Carlyle, J.M., Hock, V., McInerney, M., and Morefield, S., 2004: Mathematical Tension / Corrosion Prediction Models for Tainter Gate Tendon Rods. Final Report to the US Army Corps of Engineers, Contract DACW42-03-P-0289, US Army Construction Engineering Research Laboratory, Champaign, IL 61826-9005, 30pp.

Carlyle, J.M., Hock, V., McInerney, M., and Morefield, S., 2004: Nondestructive Testing for Service Life Prediction of Reinforced Concrete Structures. Final Report to the US Army Corps of Engineers, Contract DACA42-02-C-0020, US Army Construction Engineering Research Laboratory,Champaign, IL, 61826-9005, 107 pp.

Krautkramer, Josef and Krautkramer, Herbert, 1990: *Ultrasonic Testing of Materials*, 4th edition, Springer-Verlag, 667 pp.

Filipczynski, L., Pawlowski, Z., and Wehr, J., 1966: *Ultrasonic Methods of Testing Materials*, Butterworth & Co, 280 pp.

Ensminger, D., “Ultrasonics”, Marcel Dekker, Inc., New York, NY, 1973